Comparative study of hyperon-nucleon interactions in a quark model and in chiral effective field theory by low-momentum equivalent interactions and G matrices

M. Kohno
Physics Division, Kyushu Dental College, Kitakyushu 803-8580, Japan
(Received 9 November 2009; published 14 January 2010)

Hyperon-nucleons interactions constructed by two frameworks, the Kyoto-Niigata SU_6 quark model and the chiral effective field theory, are compared by investigating equivalent interactions in a low-momentum space and, in addition, by calculating hyperon single-particle potentials in the lowest-order Brueckner theory in symmetric nuclear matter. Two descriptions are shown to give similar matrix elements in most channels after renormalizing high momentum components. Although the range of the ΛN interaction is different in two potentials, the Λ single-particle potential in nuclear matter is very similar. The Σ-nucleus and Ξ-nucleus potentials are also found to be similar. These predictions are to be confronted with forthcoming experimental data.

DOI: 10.1103/PhysRevC.81.014003 PACS number(s): 13.75.Ev, 21.30.Fe, 21.65.−f

I. INTRODUCTION

It is basically important to obtain a realistic potential description of baryon-baryon interactions for understanding the properties of baryons and baryonic systems. Baryon-baryon interactions in the strangeness $S = -1$ and $S = -2$ sectors were not well regulated by experiments, except for a fair amount of data for Λ hypernuclei. The construction of these potentials has to rely on an underlying theoretical framework, such as a one boson-exchange potential (OBEP) picture, a constituent quark model, and a chiral effective field theory (EFT). Predictions of these different potential descriptions for hypernuclear phenomenon, for example, Σ and Ξ hypernuclear bound states, multihyperon systems, and properties of neutron star matter, naturally vary. Future experimental data will constrain the parameters to allow more solid predictions. Before the experiment, however, it is interesting and important to make a comparison between presently available potential parametrizations to elucidate the character of the underlying theoretical frameworks.

As is known in the nucleon-nucleon (NN) interaction, the direct comparison of the bare potential is not meaningful. We have to consider some effective interactions and quantities closely connected to experimental observables, such as single particle (s.p.) potentials in the nuclear medium. In this context, equivalent interactions in a low-momentum space [1] have become a useful tool to figure out the properties of baryon-baryon interactions without being obscured by uncertainties in the description of the short-range part. We call an effective interaction in a restricted space, which reproduces the same eigenvalues or T matrices in the same space as those of the original full-space interaction an equivalent interaction.

In Ref. [2], we reported the comparison of low-momentum space equivalent interactions of the Nijmegen OBEP NSC97F [3] and the Kyoto-Niigata SU_6 quark-model potential fss2 [4] for ΛN and ΣN interactions and showed the property of the ΞN interaction of fss2. For the ΛN case, two models provide very similar matrix elements in a low-momentum space, although the short-range part is considerably different. On the contrary, there is a difference in the ΣN interaction.

In this article we extend the study to consider the potential by the chiral EFT [5,6] and make a comparison with the quark-model potential fss2 in two ways; Namely by investigating equivalent interactions in a low-momentum space and hyperon s.p. potentials in nuclear matter in the framework of the lowest-order Brueckner theory. The elimination of the high-momentum components by considering low-momentum space-equivalent interaction enables us to concentrate on features of the YN interaction relevant to the low-energy experimental hypernuclear observables. To consider the implication of baryon-baryon interactions to experimental quantities, it is not sufficient to study the low-momentum interaction. Important correlations inside a low-momentum space and many-body correlations in a high momentum, including the components in a high-momentum space, have to be incorporated to obtain physically meaningful quantities. The standard way to achieve this in nuclear physics is the Brueckner theory. It deals with singular short-range parts of the baryon-baryon interaction and at the same time incorporates important many-body effects through the Pauli principle and the dispersion effects. Thus we calculate hyperon s.p. potentials in symmetric nuclear matter in the Brueckner theory. The feasible lowest-order calculation accounts for semiquantitatively the structure dependence of the hyperon-nucleon interactions in the nuclear medium. The s.p. potential is one of most important quantities connected with baryon properties in the nuclear medium, although they are not direct observables. Therefore, the hyperon s.p. potentials in the lowest order Brueckner theory (LOBT) in symmetric nuclear matter provide a further insight into the properties of the bare hyperon-nucleon interactions.

The fss2 potential is the most recent model by the Kyoto-Niigata group [4,7], in which an effective gluonic interaction and long-ranged one-boson exchanges between quarks are considered in the resonating group method (RGM) for two constituent-quark clusters. This fss2 [4] achieves comparable accuracy in the NN sector to modern realistic NN potentials. The extension of the potential to the strangeness $S = -1$ and $S = -2$ sectors on the basis of the parameters fixed in the NN sector was shown [4] to be less ambiguous than the

OBEP parametrization. In fact, the prediction of the overall repulsive nature of the Σ-nucleus potential before experiments is supported by analyses [8–10] of the (π^-, K^+) Σ production inclusive spectra [8,11]. The microscopic calculation of the Σ-nucleus s.p. potential in finite nuclei [12] further demonstrated that the fss2 potential actually reproduces the subtle structure of the weak surface attraction and the repulsion inside a nucleus, which is indicated by the analyses [13] of the shift and width of Σ^- atomic levels.

The chiral EFT potentials in the strangeness $S = -1$ and $S = -2$ sector were recently developed by the Jülich group [5,6], as the extension of the nucleon-nucleon case [14]. This description uses pseudoscalar-meson exchanges and flavor SU_3 invariant contact terms, regularized by a cutoff mass of around 600 MeV. At present the interaction is derived in the leading order. Parameters of the contact terms, five in the $S = -1$ sector and an additional one parameter in the $S = -2$ sector, are determined by fitting to available experimental data. Because the description for the short-range part is considerably different from that of fss2, it is worthwhile to compare the two potentials.

In Sec. II, we briefly describe the basics of the equivalent interaction theory in a model space. Results of numerical calculations in $^1S_0$ and $^3S_1$ channels are presented in Sec. III for ΛN, ΣN, and ΞN interactions. We also present the Λ, Σ, and Ξ s.p. potentials in symmetric nuclear matter at various Fermi momenta between $k_F = 0.75$ and 1.45 fm^{-1}. Section IV summarizes the results of the present article.

II. EQUIVALENT INTERACTION

Suzuki and Lee [15,16] proposed the basic idea to construct the energy-independent hermitian equivalent Hamiltonian in a model space P. Their consideration is closely related to the recent development of low-momentum interactions [1]. It is elementary to observe that the eigenvalues of the original Hamiltonian H do not change when H is transformed by a similarity transformation, namely by a regular matrix X and its inverse X^{-1} as $H \Rightarrow H' \equiv X^{-1}HX$. It is easy to see that if a decoupling condition $QX^{-1}HXP = 0$ holds with $Q = 1 - P$, $PX^{-1}HXP$ becomes the equivalent Hamiltonian $H_{\rm eff}$ in the model space P. Thus the task to find $H_{\rm eff}$ is reduced to determine X which satisfies $QX^{-1}HXP = 0$. It is sufficient first to consider a regular matrix X in the following form

$$X = \begin{pmatrix} 1, & 0 \\ \omega, & 1 \end{pmatrix}, \quad \text{then} \quad X^{-1} = \begin{pmatrix} 1, & 0 \\ -\omega, & 1 \end{pmatrix}. \tag{1}$$

The mapping matrix $\omega = Q\omega P$, which connects the P and Q spaces, plays a central role in the construction of $H_{\rm eff}$. The decoupling condition $QX^{-1}HXP = 0$ now reads

$$QHP + QHQ\omega - \omega PHP - \omega PHQ\omega = 0. \tag{2}$$

Because this is a nonlinear equation for ω, we have to use some iteration method to solve it. Determining the mapping operator ω, we obtain an energy-independent equivalent Hamiltonian in the model space P as $H_{\rm eff} = PHP + PHQ\omega P$. This equivalent Hamiltonian is not Hermitian at this stage. If we utilize a unitary matrix $\tilde{X}$ in the following Okubo form [17] constructed from ω of Eq. (1) to transform the original H, we obtain the Hermitian Hamiltonian.

$$\tilde{X} = \begin{pmatrix} 1, & -\omega^\dagger \\ \omega, & 1 \end{pmatrix} \begin{pmatrix} 1 + \omega^\dagger\omega, & 0 \\ 0, & 1 + \omega\omega^\dagger \end{pmatrix}^{-1/2}, \tag{3}$$

Subtracting the kinetic part, we can define an equivalent interaction in the model space. In the case of the equivalent interaction in a two-body problem, for example, the elimination of high-momentum components, the procedure is transparent because many-body correlations do not appear.

The actual calculation of the mapping operator ω is carried out by method 2 in Ref. [18]. The extension to the hyperon-nucleon case, in which several baryon-channels couple each other and there appears an antisymmetric spin-orbit coupling absent in the NN interaction, is straightforward. However, we encounter numerical troubles in some cases (i.e., in the $T = \frac{1}{2}$ ΣN $^1S_0$ and $^3S_1$ channels and the $T = 0$ ΞN $^1S_0$ channel) when the threshold of another baryon channel is located in the low-momentum space. The extended method 2 yields oscillatory behavior of the matrix elements of the equivalent interaction as a function of the momentum that varies as mesh points are altered. One tentative remedy is to use rather coarse mesh points to obtain smooth k dependence. However, this does not always work. It requires, in the future, a new numerical method or a more radical reformulation such as introducing a channel-dependent cutoff [19] to resolve the problem. Because the aim of the present evaluation is to compare characters of different baryon-baryon interactions and not to do exact structure calculations on the basis of the low-momentum equivalent interaction, we present the results with the oscillatory behavior in case it appears.

G-matrix calculations for hyperons in symmetric nuclear matter are carried out using the continuous prescription for intermediate spectra. Hyperon s.p. potentials are determined self-consistently. Details are reported in Ref. [20]. In calculating the hyperon-nucleon G matrices for chiral EFT, we use the nucleon s.p. potential obtained by fss2 to focus on the properties of the hyperon-nucleon interactions.

III. CALCULATED RESULTS

We calculate equivalent ΛN, ΣN, and ΞN matrix elements in the low-momentum space with the cutoff value of $\Lambda = 2.0$ fm^{-1} for the $^1S_0$ and $^3S_1$ partial waves, starting from the Kyoto-Niigata SU_6 quark-model potential fss2 [4] and the chiral EFT potential [5,6]. This momentum scale should be regarded as a representative one for which the potential dependence of the description of high-momentum components has been shown [1] to disappear in the case of the NN interaction. As explained in Ref. [2], we use the energy-independent version of the quark-model potential [21] that eliminates the energy dependence originating the RGM treatment of the quark clusters. Note that the short-range part of the baryon-baryon interaction in the quark model is constructed by an RGM framework for nonrelativistic quark-clusters, while that of the chiral EFT potential is influenced by the contact terms determined by phenomenological fitting.

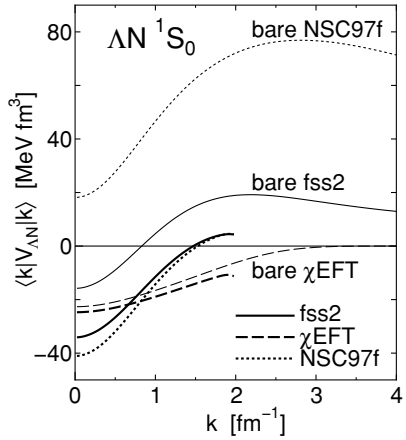

FIG. 1. Diagonal matrix elements of the equivalent interaction in the low-momentum space with $\Lambda = 2$ fm^{-1} for the ΛN $^1S_0$ channel, using the quark-model potential fss2 [4], the Nijmegen potential NSC97 [3], and the chiral EFT potential (χEFT) [5] with a cutoff mass of 600 MeV. Bare matrix elements are shown by thin curves.

A. ΛN interaction

Figures 1 and 2 show the low-momentum space diagonal matrix elements of the equivalent ΛN interaction in the $^1S_0$ and $^3S_1$ channels, respectively, together with bare matrix elements. In this case we include the equivalent interaction of the Nijmegen potential NSC97f [3], in addition to the quark model potential fss2 [4], and the chiral EFT potential [5] with a cutoff mass of 600 MeV.

As reported already in Ref. [2], the NSC97f and the fss2 provide very similar matrix elements in the low-momentum space, in spite of the large difference in the short-range part as the bare matrix elements indicate. However, the k dependence of the chiral EFT potential differs from the other two potentials, though the overall attractive strength is of the same order. As a result of the regularization with the cutoff mass of 600 MeV, the high-momentum component of the chiral EFT potential is small and the equivalent interaction is not so much different from the bare interaction in the low-momentum space. The weak k dependence suggests that the chiral EFT interaction is more short-ranged than other two potentials in both the

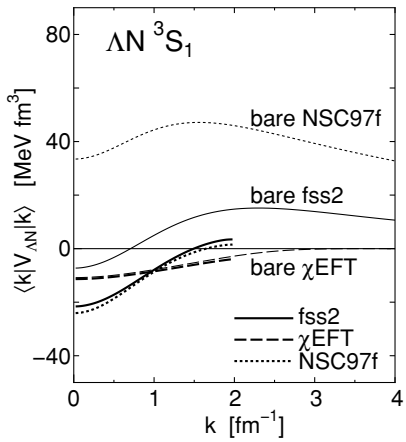

FIG. 2. Same as Fig. 1, but for the ΛN $^3S_1$ channel.

$^1S_0$ and $^3S_1$ channels. Note that in the ΛN case, a direct isovector π exchange process is absent. In the $^3S_1$ channel, a considerable amount of the attractive contribution is expected from the ΛN–ΣN coupling through the π exchange. In the cases of fss2 and NSC97f, the attraction in a low-momentum space comes from this coupling in a high-momentum space with the tensor component of the π exchange. In contrast, the small difference between bare and low-momentum space matrix elements in the case of chiral EFT implies that the coupling effect in a high-momentum space is incorporated in the parameter of the contact terms.

Diagonal matrix elements of the effective interaction in momentum space determine baryon s.p. potentials in nuclear matter. Because properties of the s.p. potential can be more directly inferred from experimental data, it is useful to present the calculated Λ s.p. potential from the ΛN interaction. We can consider the Hartree potential obtained by the equivalent interaction in the low-momentum space. However, we prefer to use the standard LOBT in which some important many-body effects are incorporated. The calculated Λ s.p. potential from the two bare potentials, fss2 and chiral EFT, are shown in Fig. 3. The real part is very similar in its magnitude and k_F dependence. It is not easy to detect the difference of the k dependence observed in the equivalent interactions in the $^1S_0$ and $^3S_1$ channels. The imaginary part of the s.p. potential indicates the strength of the ΛN–ΣN coupling. At low momentum, the chiral EFT potential gives slightly larger imaginary strength. The weaker imaginary potential from the chiral EFT than that from fss2 at a large k region is due to the weak ΛN–ΣN coupling inherent in the cutoff mass of 600 MeV. As noted earlier, the coupling effect at a high-momentum region may be renormalized into the parameter of the contact terms in the chiral EFT potential and thus the explicit ΛN–ΣN coupling at the large momentum region is weak in this parametrization.

As a whole, three bare potentials, fss2, NSC97f, and chiral EFT, for the ΛN interaction provide similar descriptions of the Λ s.p. potential. In the literature [22–24] we find that the energy of the hypertriton is well reproduced by three potentials: namely $E^{^3_\Lambda H} = -2.30$, -2.487, and -2.34 MeV for NSC97f, fss2, and chiral EFT, respectively, compared with the empirical value of -2.354 ± 0.050 MeV. However, the difference observed in Figs. 1 and 2 for the k dependence of the equivalent interaction is probably detectable in some experimental observables.

Finally, it is worth commenting on an unresolved problem of the microscopic understanding of the small Λ s.p. spin-orbit potential. Experimentally, it was established [25] that the spin-orbit splitting of the Λ s.p. levels in nuclei is very small. It is helpful to consider the Scheerbaum factor S_Λ [26] calculated in nuclear matter to relate the strength of the Λ-nucleus spin-orbit potential to the two-body ΛN interaction. The Λ-nucleus s.p. potential is well simulated by

$$U_\Lambda^{\ell s}(r) = -\frac{\pi}{2} S_\Lambda \frac{1}{r} \frac{d\rho(r)}{dr} \boldsymbol{\ell\sigma}, \tag{4}$$

where $\rho(r)$ is a nucleon density distribution. The necessary value of S_Λ to explain the experimental data is about -3.2 MeV fm^5. In contrast, three potentials considered here

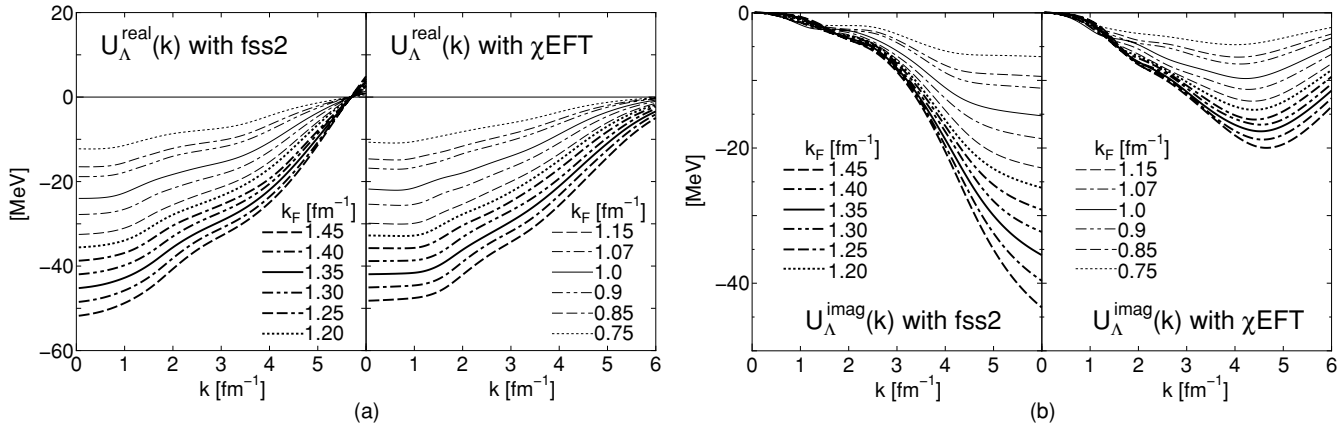

FIG. 3. Momentum dependence of Λ s.p. potential in symmetric nuclear matter at various Fermi momenta k_F: (a) real part and (b) imaginary part. The calculations are in the LOBT with the continuous prescription for the intermediate spectra. The left panel shows the result of the quark-model potential fss2 [4] and the right panel those of the potential of the chiral EFT (χEFT) [5] with a cutoff mass of 600 MeV.

give $S_\Lambda = -15.4$, -12.2, and $+4.8$ MeV fm^5 for NSC97f, fss2, and chiral EFT, respectively, in normal symmetric nuclear matter, namely $k_F = 1.35$ fm^{-1}. The quark model suggests that an antisymmetric spin-orbit component of the two-body spin-orbit interaction may be important to cancel the ordinary spin-orbit interaction. However, this mechanism does not work quantitatively in fss2. The other two potentials do not contain the antisymmetric spin-orbit component. It is significant that the chiral EFT potential predicts an opposite sign for the Λ s.p. spin-orbit potential in the present leading order construction.

B. ΣN interaction

Figure 4 shows the low-momentum space diagonal matrix elements of the equivalent ΣN interaction in the $^1S_0$ and $^3S_1$ channels for the isospin $T = 1/2$ and $3/2$, respectively, together with bare matrix elements for the quark-model potential fss2 [4] and the chiral EFT potential with the cutoff mass of 600 MeV.

It is notable that the equivalent interactions of the quark model fss2 and the chiral EFT potential are very similar except for the $^3S_1$ $T = 1/2$ channel. It is known that the ΣN $^1S_0$ $T = 3/2$ state consists of the same $(2, 2)$ flavor SU_3 symmetric component of the Elliott notation (λ, μ) as the NN $^1S_0$ state. Thus, this channel is expected to hold a rather strong attraction. This character is manifested in the $J^\pi = 0^+$ $^4_\Sigma$He bound state seen in the ^{4}He(K^-, π^-) reactions [27,28]. The chiral EFT potential also has this attraction, although the k dependence is gentle as in the ΛN-equivalent interactions.

The quark model picture is known from earlier studies [7,29] to give a definite prediction that the ΣN $^3S_1$ $T = 3/2$ state should be strongly repulsive due to the quark Pauli effect, which has no explicit counterpart in the OBEP parametrization. The repulsive character persists in the low-momentum space. Owing to the spin and isospin weight factors, this $^3S_1$ $T = 3/2$ state dominantly contributes to the Σ s.p. potential in the nuclear medium, as will be explicitly shown in the calculated Σ s.p. potential. Analyses [8–10] of the (π^-, K^+) Σ formation inclusive spectra [8] supported

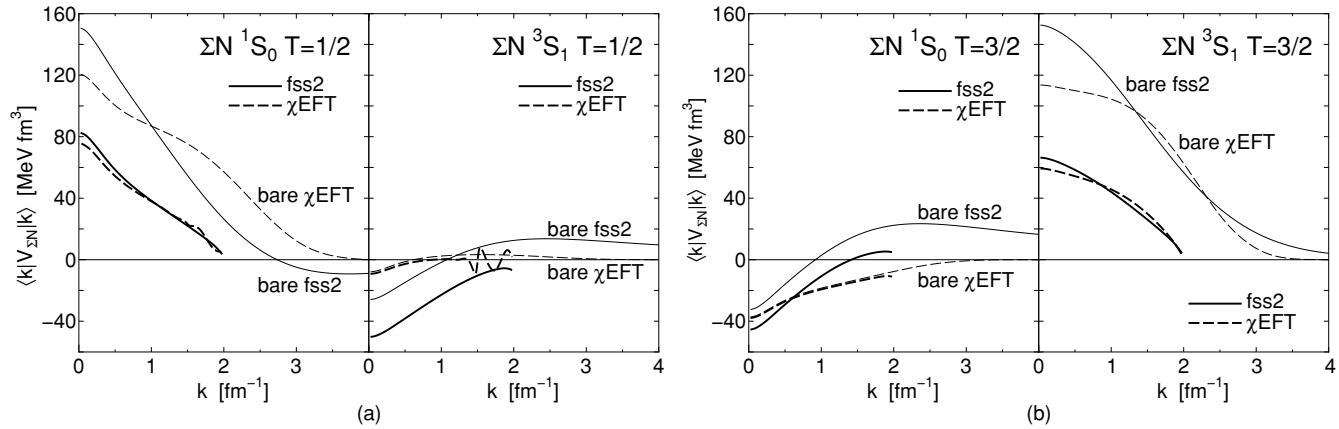

FIG. 4. Diagonal matrix elements of the equivalent interaction in the low-momentum space with $\Lambda = 2$ fm^{-1} for the ΣN $^1S_0$ and ΣN $^3S_1$ channels, using fss2 [4] and chiral EFT (χEFT) [5]: (a) isospin $T = 1/2$ and (b) $T = 3/2$.

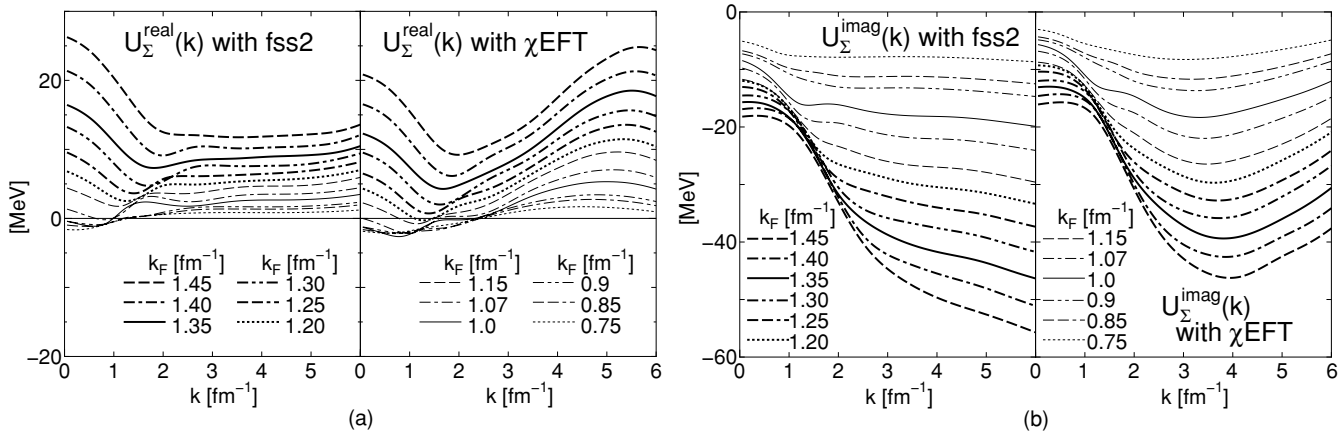

FIG. 5. Same as Fig. 3, but for the Σ s.p. potential.

the overall repulsive nature of the Σ-nucleus potential. Note that the actual calculation [12] in finite nuclei shows that we obtain weak attractive potential at the surface region of nuclei that is necessary to account for the energy shift of Σ^- atomic levels.

It is interesting to see that the matrix elements in the $^3S_1$ $T = 3/2$ channel are similar for the fss2 and the chiral EFT. While the repulsive character is dictated by the quark Pauli effect in the fss2, the parameter of the contact term determined phenomenologically is responsible for this repulsion in chiral EFT.

Calculated Σ s.p. potentials in symmetric nuclear matter are shown in Fig. 5. Two potentials predict very similar patterns for the real part both in the k dependence and in the k_F dependence. The size of the imaginary strength is also seen to be in resemblance except for the region beyond $k \sim 4$ fm^{-1}.

C. ΞN interaction

Figure 4 shows the low-momentum space equivalent ΞN interaction in the $^1S_0$ and $^3S_1$ channels for the isospin $T = 1/2$ and $3/2$, respectively, together with the bare matrix elements up to $k = 4$ fm^{-1}. In the $T = 1$ channel, two potentials have similar repulsive characters both in the bare and equivalent interactions.

The quark-model potential provides fair attraction in the $T = 0$ $^1S_0$ channel. The largest part of this attraction comes from the ΞN–$\Lambda\Lambda$–$\Sigma\Sigma$ coupling. This can be checked by observing that, if we switch off the baryon-channel coupling, the matrix elements are close to those of the bare interaction. In such a situation, it is important to consider the effect of the baryon-channel coupling in the P space to obtain more physically meaningful information. The situation is the same in chiral EFT, though the resulting attraction is very small in magnitude. Note that in the chiral EFT theory an additional parameter has to be introduced in the $^1S_0$ channel when extending to the $S = -2$ sector from the $S = -1$ sector.

The $^3S_1$ $T = 0$ state is classified to the pure $(11)_a$ state in the flavor SU_3 symmetry and no baryon-channel coupling appears in this state. The quark model [4] predicts that the bare ΞN interaction is already weak. Figure 6(a) shows that the low-momentum equivalent ΞN interaction in this partial wave becomes slightly attractive.

The quark-model potential fss2 [4] predicts that the ΞN interactions in $^3S_1$ channels are weak. For the estimation of the Ξ-nucleus s.p. potential in the nuclear medium, we expect an

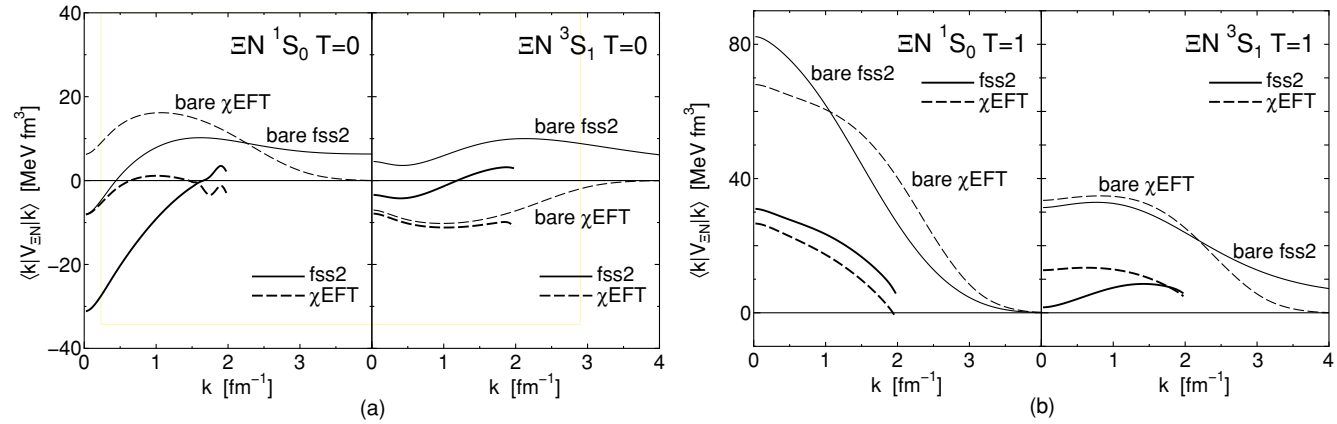

FIG. 6. Same as Fig. 4, but for the ΞN $^1S_0$ and ΞN $^3S_1$ channels: (a) isospin $T = 0$ and (b) isospin $T = 1$. The chiral EFT (χEFT) potential is from Ref. [6].

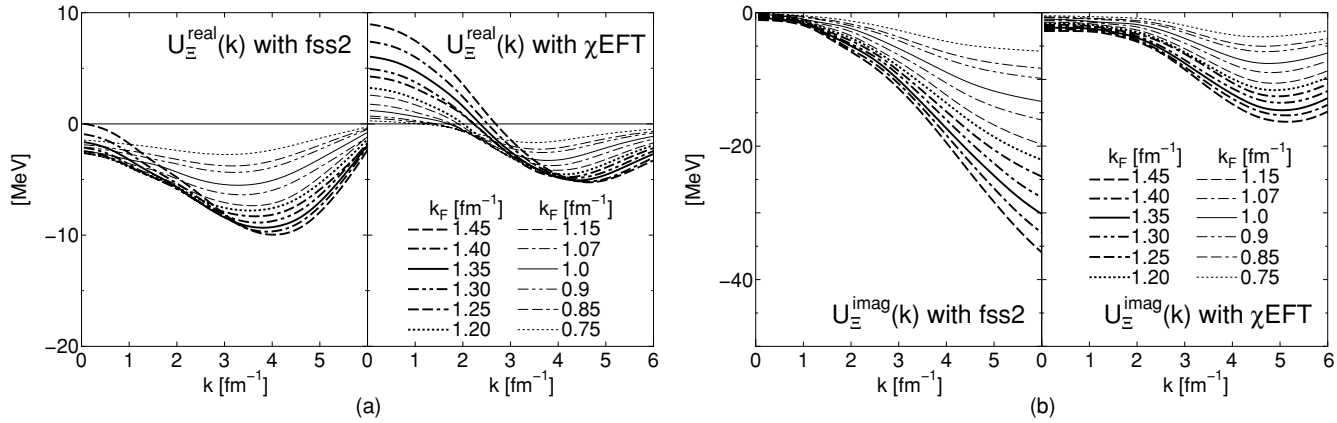

FIG. 7. Same as Fig. 3, but for the Ξ s.p. potential. The chiral EFT (χEFT) potential is from Ref. [6].

attractive contribution from the ${}^1S_0$ $T = 0$ state, but a repulsive contribution from the ${}^1S_0$ $T = 1$ state. Higher partial waves can influence the sign of the Ξ-nucleus s.p. potential, although it is unlikely that they bring about sizable net attractive or repulsive contributions. The calculated Ξ s.p. potentials in symmetric nuclear matter in the LOBT are shown in Fig. 7. The potential from the fss2 is seen to be weak. The tendency that the attractive strength is largest at $k = 3 \sim 4$ is owing to the net contribution of ΞN p waves.

Although the potential is attractive in infinite matter, the calculation in finite nuclei [12] shows that the Ξ s.p. potential is weakly attractive at the nuclear surface and oscillates around zero inside the nucleus. Judging from Fig. 7, a more repulsive Ξ s.p. potential in finite nuclei is expected from chiral EFT. The presently available (K^-, K^+) spectrum [30] at the Ξ^- production threshold region is shown in Ref. [31] to be consistent with the weakly repulsive Ξ potential. The prediction is soon to be confronted with experimental data with better accuracy obtained from Japan Proton Accelerator Research Complex (J-PARC) [32].

IV. SUMMARY

We compare two descriptions of the hyperon-nucleon interactions, the Kyoto-Niigata quark-model potential fss2 [4] and the chiral EFT potential [5,6], by calculating low-momentum space equivalent interactions and hyperon s.p. potentials in the LOBT in symmetric nuclear matter obtained from these bare potentials. The purpose is to elucidate the similarity and the difference in the ΛN, ΣN, and ΞN interactions between the quark model and the chiral EFT theory. The former model is based on a resonating group method for two constituent-quark clusters with an effective gluonic interaction and long-ranged one-boson exchanges between quarks. The energy dependence inherent in the RGM treatment is eliminated by the method in Ref. [21]. The latter parametrization uses pseudoscalar-meson exchanges and flavor SU_3 invariant contact terms, regularized by a cutoff mass of around 600 MeV. Parameters of the contact terms, five in the $S = -1$ sector and an additional one parameter in the $S = -2$ sector, are determined by fitting to available experimental data. Because of the difference in the description for the short-range part, it is worthwhile to compare the two potentials.

In the previous article [2], we showed that the ΛN-equivalent interaction in the low-momentum space is almost identical for the quark model fss2 and the Nijmegen OBEP model NSC97f [3]. In this article, we find that the leading order chiral EFT interaction gives matrix elements of the equivalent interaction, which have different k dependence from fss2. This difference is not visible in the Λ s.p. potential in the nuclear medium, although it will probably be detectable in some observables in future experiments. Note that there is an unresolved problem of describing very small spin-orbit splitting of the Λ hyperon in nuclei. G-matrix calculations, in which the effects of the ΛN–ΣN coupling in the nuclear medium are taken care of, show that fss2 does not provide a small Λ-nucleus spin-orbit potential necessary to account for the empirical data, in spite of the tendency of the cancelation of the ordinary and antisymmetric spin-orbit components. However, the chiral EFT potential, having no antisymmetric spin-orbit component, predicts a small but opposite sign for the spin-orbit potential. It will be interesting if the effects of the next leading order corrections are revealed in future analysis.

As for the ΣN interactions, the quark model fss2 and the chiral EFT potential mostly give similar matrix elements of the equivalent interactions in a low-momentum space, except for the ${}^3S_1$ $T = 1/2$ state. It is interesting to see that the repulsion in the ${}^3S_1$ $T = 3/2$ state predicted by the quark model as a result of the quark Pauli effect is reproduced as well in the chiral EFT parametrization. This similarity reflects in that calculated Σ s.p. potentials in symmetric nuclear matter also resemble in their magnitude, momentum dependence, and k_F dependence. The prediction of the repulsive potential for the Σ hyperon embedded in the nuclear medium is not common among several baryon-baryon interaction parametrizations. Therefore, checks by forthcoming experiments, for example, in the J-PARC project [32], will be very important for understanding the ΣN interaction.

The resemblance of the two interactions also holds in the ΞN interaction. The fss2 interaction provides weakly attractive s.p. potentials in symmetric nuclear matter. The chiral EFT interaction tends to give slightly more repulsive s.p.

potentials as a result of the lack of attraction in the ${}^1S_0$ $T = 0$ channel. The microscopic calculation [12] of the Ξ-nucleus potential in finite nuclei shows that the fss2 predicts an almost zero potential. At the surface region, the potential is weakly attractive and inside the nucleus the potential fluctuate around zero. Such a weak Ξ-nucleus potential is shown in Ref. [31] to be able to account for the existing (K^-, K^+) spectrum at the threshold region [30]. These experimental data are based on the small number of counts and thus may not be accurate enough to conclude the strength of the Ξ-nucleus potential. We expect new Ξ-production spectrum data with better accuracy from the J-PARC experiments [32], which will provide important information on the baryon-baryon interaction in the $S = -2$ sector.

ACKNOWLEDGMENTS

The author is grateful to Y. Fujiwara, H. Polinder, and J. Haidenbauer for providing him with computational codes of their baryon-baryon interactions.

[1] S. K. Bogner, T. T. S. Kuo, and A. Schwenk, Phys. Rep. **386**, 1 (2003).
[2] M. Kohno, R. Okamoto, H. Kamada, and Y. Fujiwara, Phys. Rev. C **76**, 064002 (2007).
[3] T. A. Rijken, V. G. J. Stoks, and Y. Yamamoto, Phys. Rev. C **59**, 21 (1999).
[4] Y. Fujiwara, Y. Suzuki, and C. Nakamoto, Prog. Part. Nucl. Phys. **58**, 439 (2007).
[5] H. Polinder, J. Haidenbauer, and Ulf-G. Meißner, Nucl. Phys. **A779**, 244 (2006).
[6] H. Polinder, J. Haidenbauer, and Ulf-G. Meißner, Phys. Lett. **B653**, 29 (2007).
[7] Y. Fujiwara, C. Nakamoto, and Y. Suzuki, Phys. Rev. Lett. **76**, 2242 (1996).
[8] H. Noumi *et al.*, Phys. Rev. Lett. **89**, 072301 (2002); **90**, 049902(E) (2003).
[9] T. Harada and Y. Hirabayashi, Nucl. Phys. **A759**, 143 (2005).
[10] M. Kohno, Y. Fujiwara, Y. Watanabe, K. Ogata, and M. Kawai, Phys. Rev. C **74**, 064613 (2006).
[11] P. K. Saha *et al.*, Phys. Rev. C **70**, 044613 (2004).
[12] M. Kohno and Y. Fujiwara, Phys. Rev. C **79**, 054318 (2009).
[13] C. J. Batty, E. Friedman, and A. Gal, Phys. Lett. **B335**, 273 (1994); Phys. Rep. **287**, 385 (1997).
[14] E. Epelbaum, W. Glöckle, and Ulf-G. Meißner, Nucl. Phys. **A747**, 362 (2005).
[15] K. Suzuki and S. Y. Lee, Prog. Theor. Phys. **64**, 2091 (1980).
[16] S. Y. Lee and K. Suzuki, Phys. Lett. **B91**, 173 (1980).
[17] S. Okubo, Prog. Theor. Phys. **12**, 603 (1954).
[18] S. Fujii, E. Epelbaum, H. Kamada, R. Okamoto, K. Suzuki, and W. Glöckle, Phys. Rev. C **70**, 024003 (2004).
[19] M. Wagner, B.-J. Schaefer, J. Wambach, T. T. S. Kuo, and G. E. Brown, Phys. Rev. C **74**, 054003 (2006).
[20] M. Kohno, Y. Fujiwara, T. Fujita, C. Nakamoto, and Y. Suzuki, Nucl. Phys. **A674**, 229 (2000).
[21] Y. Suzuki, H. Matsumura, M. Orabi, Y. Fujiwara, P. Descouvemont, M. Theeten, and D. Baye, Phys. Lett. **B659**, 160 (2008).
[22] K. Miyagawa, H. Kamada, W. Glöckle, and V. Stoks, Phys. Rev. C **51**, 2905 (1995).
[23] A. Nogga, *Proceedings of Chiral Dynamics 2006* (World Scientific, Singapore, 2007).
[24] Y. Fujiwara, Y. Suzuki, M. Kohno, and K. Miyagawa, Phys. Rev. C **77**, 027001 (2008).
[25] O. Hashimoto and H. Tamura, Prog. Part. Nucl. Phys. **57**, 564 (2006).
[26] R. R. Scheerbaum, Nucl. Phys. **A257**, 77 (1976).
[27] R. S. Hayano *et al.*, Phys. Lett. **B231**, 355 (1989).
[28] T. Nagae *et al.*, Phys. Rev. Lett. **80**, 1605 (1998).
[29] M. Oka, K. Shimizu, and K. Yazaki, Nucl. Phys. **A464**, 700 (1987).
[30] P. Khaustov *et al.*, Phys. Rev. C **61**, 054603 (2000).
[31] M. Kohno and S. Hashimoto, Prog. Theor. Phys. **123** (2010) (in print).
[32] T. Nagae, Nucl. Phys. **A805**, 486 (2008).